

Campaign report

August 2022

IceBird Summer 2022 Campaign

**Sea ice surveys with Polar 6 from
Station Nord**



Authors

Thomas Krumpen Alfred Wegener Institute
Gerit Birnbaum Helmholtz Centre for
Valentin Ludwig Polar and Marine Research
Christoph Petersen Bremerhaven

This work was funded by the
Federal Ministry of Education and Research

IceBird Summer 2022 campaign

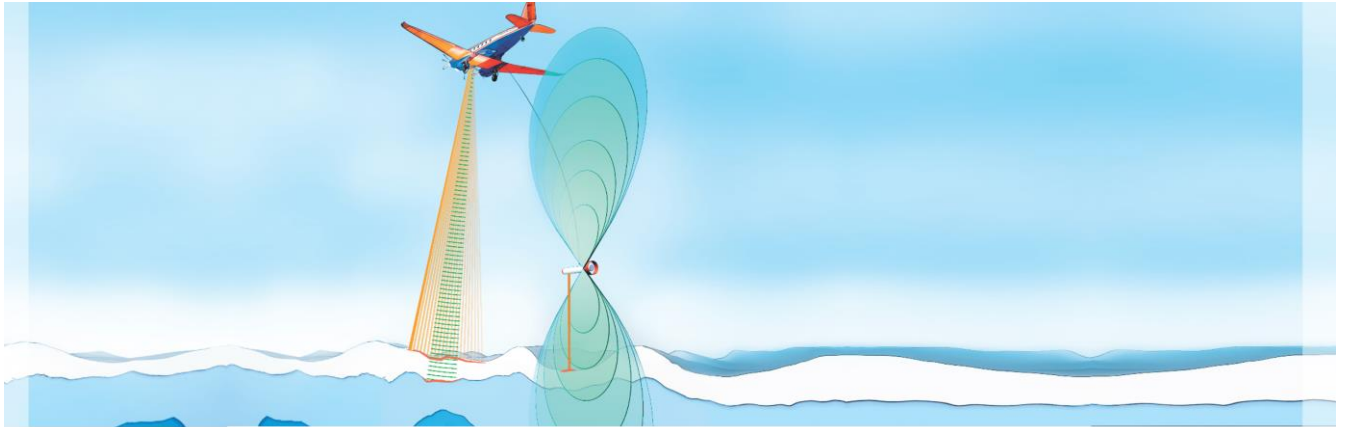
| Campaign overview | |
|-------------------|--|
| Base | Station Nord |
| Route | Bremen - Longyearbyen – Station Nord – Longyearbyen - Bremen |
| Duration | August 02 –August 24, 2022 |
| Exp. Permit | C-22-843 |
| Survey hours | 33 |
| Aircraft | Polar 6 |
| Crew | Dean Emberly (chief pilot), Alex De Boer (second pilot), Kevin Riehl (mechanic), |
| Science | Christoph Petersen (engineer), Valentin Ludwig (scientist), Gerit Birnbaum (scientist), Thomas Krumpfen (lead) |

Table of Content

- 1. Objectives**
 - Background.....
 - Long-term objectives and scientific focus in summer 2022.....
- 2. Methods and Sensors**
 - Survey flight organization and pattern
 - Weather routing and ice information
 - Instrumentation
- 3. Campaign Overview.....**
 - General weather conditions.....
 - Overview map, flight hours and active sensors
- 4. Preliminary Results.....**

Appendix:

- Survey Flight Descriptions.....**



1.0 Objectives

Changes in Arctic sea ice thickness are the result of complex interactions of the dynamic and variable ice cover with atmosphere and ocean. The availability of satellite-based estimates of Arctic-wide sea ice thickness changes is limited to the winter months. However, in light of recent model predictions of a nearly ice-free Arctic in summer and to understand the role of sea ice for the causes and consequences of a warming climate, long-term and large-scale sea ice thickness and surface observations during the melt season are more important than ever.

The AWI airborne sea ice survey program '[IceBird Summer](#)' aims to close this gap by conducting regular measurements over sea ice in summer in key regions of the Arctic Ocean. The survey program comprises and continues all airborne ice thickness measurements obtained since 2001 in the central Arctic, Fram Strait and the last ice area. The objective is to ensure the long-term availability of a unique data record of direct sea ice thickness and surface state observations (deliverable of *AWI research program POFIV, Topic 2.1: Warming Climates*). Sea ice thickness measurements are obtained with a tethered electromagnetic sensor, the AEM-Bird. Jointly with the ice thickness measurements, optical and laser systems are operated to derive sea ice surface models and melt pond distribution.

Long-term objectives of IceBird and scientific focus in Summer 2022

The survey flights are intended to repeat flight tracks of previous years and thereby to provide insight into long-term variability and trends in ice thickness and ice surface over the past two decades (e.g. Krumpfen et al. 2019). In addition, survey flights help to answer scientific questions such as the influence of 'Atlantification' on sea ice retreat (e.g. Belter et al. 2021) or the coupling between surface roughness and melt pond coverage. Data collected during IceBird Summer 2022 will be made available to the scientific community for validation of satellite retrievals from CryoSat-2 (sea ice thickness, Landy et al. 2022), TerraSAR-X and Sentinel-1 (ice type classification), and as input for improvements of numerical models and forecasting systems operated in-house (FESOM / SIDFEx) or by project partners.

2.0 Methods and Sensors

Survey flight organization and pattern

During IceBird 2022 the aircraft called Polar 6 was operated from Station Nord in Greenland. To extend the flight range of Polar 6, IceBird Summer is designed as a lightweight campaign. Therefore, instrumentation is limited to the AEM-Bird, laser scanners, optical cameras and radiation sensors. Along flight tracks, CALIB buoys were deployed for repeated surveys in the following winter (IceBird Winter 2023).

Survey flights were mostly made towards one or more pre-defined points of return. The point of return and profile length are chosen according to fuel capacity, weather condition, and ice condition. The observation of ice thickness and morphology with an AEM-Bird and scanning laser altimeter is carried out at low flight levels (50 feet, Fig. 1), The conditions of the sea ice surface are documented with a photogrammetric system and a hyperspectral camera on the way out and back in (at 2000 ft).

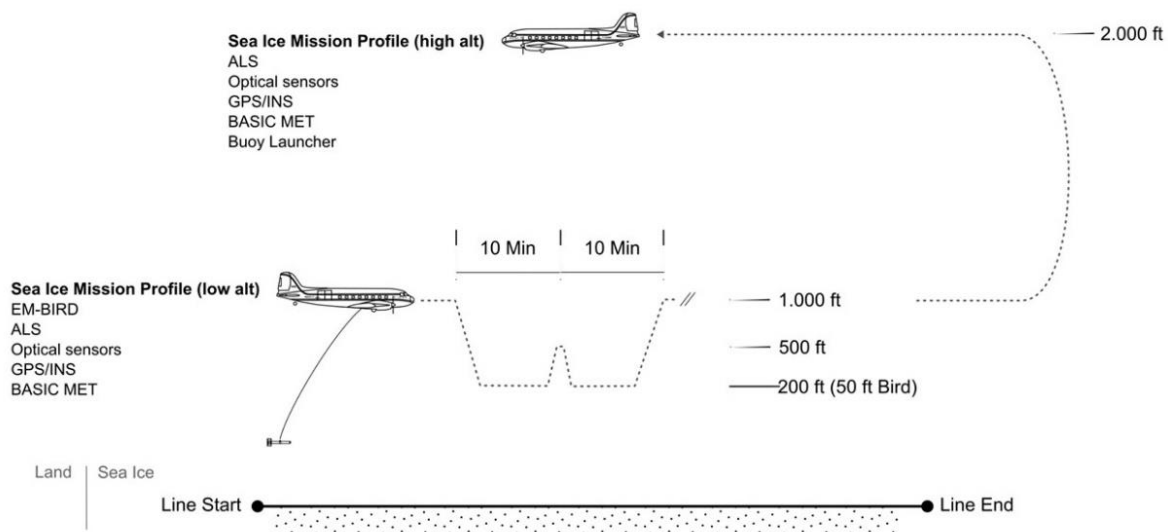


Fig. 1: Flight pattern for survey flights over sea ice.

Weather Routing and Ice Information

Weather information were obtained via SFTP from the German Weather Service (DWD). The DWD provided a tailored collection of meteograms and EPS-grams (120h ahead; initialized 00UTC and 12UTC, available with 6-9h delay, Fig. 2) for different key locations, data from weather satellites (see chapter 5.0) as well as forecast maps for cloud cover (low, medium, high), near-surface temperature, humidity, pressure and winds. All of these parameters were provided from the ECMWF forecast system, most also from the ICON system, and some in addition from the GFS system. Data download was handled in near-real time by a python script written by Valentin Ludwig. The source code is made available for future campaigns via a Git repository (<https://gitlab.awi.de/vludwig/ICEBIRD>).

Near-real time sea ice information (sea ice concentration, drift forecasts and Sentinel-1 imagery, Fig. 3) were obtained via the <https://icysea.app/> developed by [DriftNoise.com](https://driftnoise.com). In addition, a script (FramSat) kept downloading and processing newly acquired Sentinel-1 images over the survey area between August 1st and August 22nd.

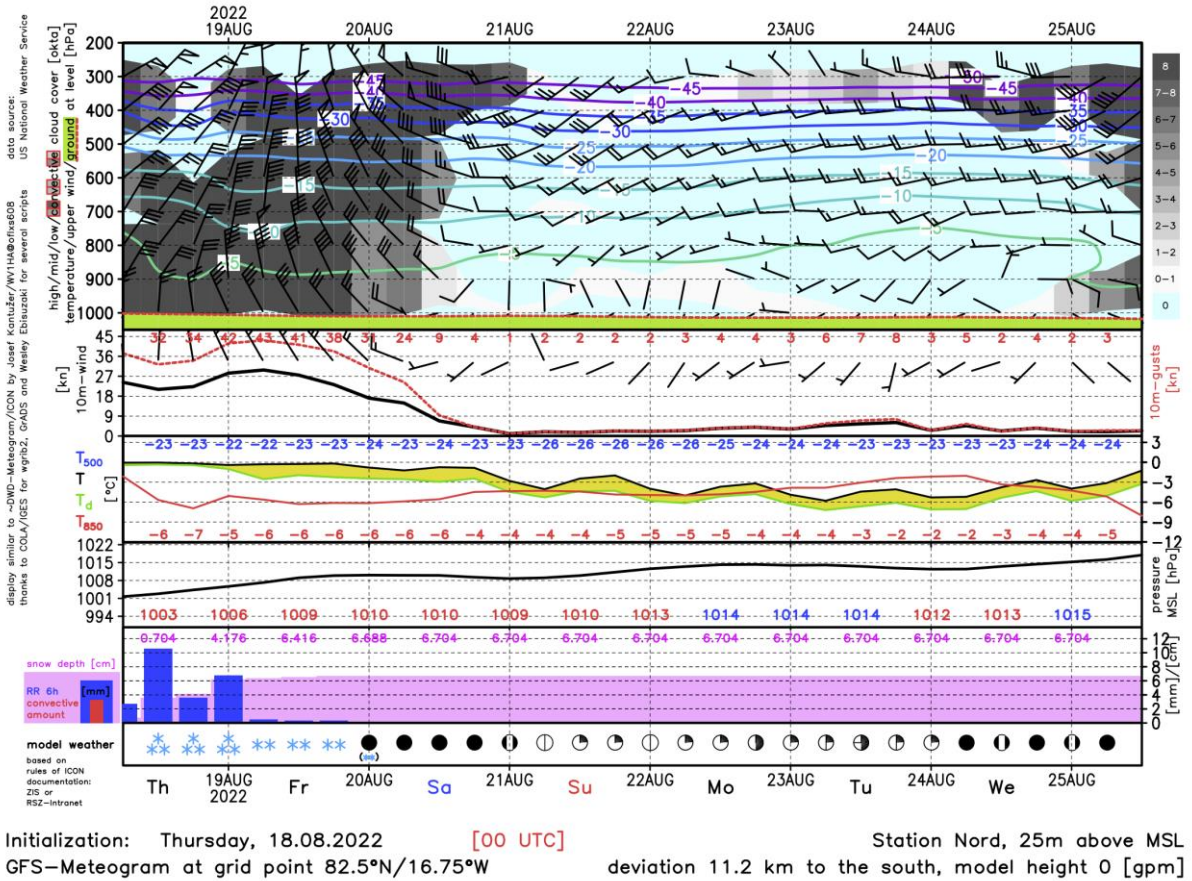


Fig. 2: Example for a GFS meteo-gram provided by the DWD for Station Nord on August 18, 2022.

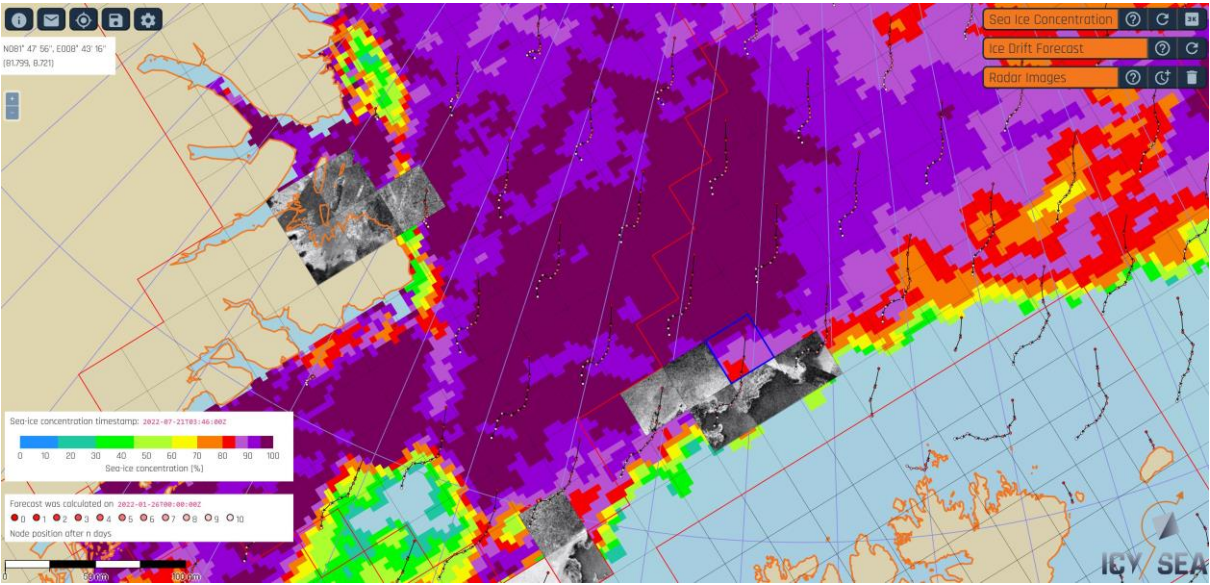


Fig. 3: Screenshot of the IcySea.app providing sea ice concentration, drift forecast and high resolution SAR images (example for 4th August)

Instrumentation

The **Specim AisaEAGLE and AisaHAWK** are sensor systems for VNIR and SWIR hyperspectral imaging. The AisaEAGLE is a pushbroom sensor covering the spectrum 400-970nm. AisaHAWK is covering the 970-2450nm range. Furthermore, the Aisa system consists of an own GPS/INS and a data acquisition unit. The AisaEAGLE has 1024 spatial pixels, 260 spectral pixels and a maximum spectral resolution of 2.4nm. The AisaHAWK has 320 spatial pixels, 244 spectral pixels and a maximum spectral resolution of 8nm.

The two **Ocean Optics QE65000** and two **NIRQuest spectrometers** are installed to measure downwelling and upwelling spectral irradiance in the wavelength range 200-1000nm and 900-2500nm, respectively. The fibre optics sensors are installed at the cabin roof looking upward and in the floor compartment looking downward.

The **MACS** (Modular Aerial Camera System) is a photogrammetric camera developed by DLR's Institute of Optical Sensor Systems. It consists of a computing unit and a sensor head. The sensor head is equipped with matrix array CCD/CMOS/thermal-infrared cameras and is mounted in the fuselage providing free view down. In order to fulfill respective application requirements, sensors, their geometry and spectral ranges are modified. Thus, particular conditions are considered, e. g., flying over brightly reflecting snow, acquisition of highly structured terrain or low flight altitudes without gaps of recorded ground surface. Currently the maximum continuous image acquisition rate is 4 frames per second enabling more than 60% overlap from an altitude of 100m (AEM-Bird surveying height).

The **Airborne electromagnetic (AEM) Bird** (AEM-Bird) is a sensor system that is towed by the research aircraft Polar-5 or Polar-6 at 20m above the ice surface. The EM sensor utilizes the contrast of electrical conductivity between sea water and sea ice to determine the distance of the instrument to the ice-water interface. An additional laser altimeter mounted inside the AEM-Bird provides the distance to the snow/ice surface. The difference between AEM and laser distance measurements is the ice plus snow thickness with an accuracy in the order of $\pm 0.1\text{m}$ over level sea ice. The so-retrieved thickness data enables us to determine the general thermodynamic and dynamic boundary conditions of ice formation. The most frequently occurring ice thickness, the mode of the distribution, represents level ice thickness and is the result of winter accretion and summer ablation.

3.0 Survey overview

Sea ice extent, weather conditions and flight activities

As of the middle of the campaign, on August 16, the Arctic-wide sea ice extent was 6.01 million square kilometers. This is below the 1981 to 2010 average, yet it is higher than in the record years 2007, 2012 and 2016. The sea ice extent in Fram Strait was higher than during previous campaigns.

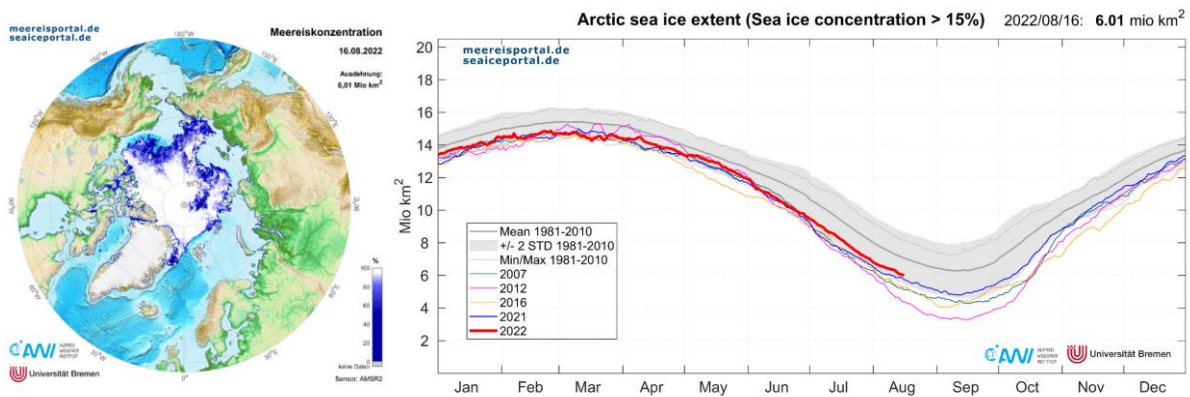


Fig. 4: Sea ice concentration (left) and extent (right) on August 16, 2022 (source: Meereisportal.de)

Unfavorable flight conditions in the vicinity of the station and/or over sea ice (low visibility / low ceiling, etc) prevented any kind of surveying activities between the date of arrival at Station Nord and August 11. Hereafter, southerly winds pushed the pack ice offshore and resulted in an opening of leads along the northern coast of Greenland. Furthermore, offshore winds led to the development of a fog- and low-level cloud free corridor at the northern tip of Greenland, slowly moving east (Fig. 5 left). As a consequence, four survey flights between August 12 to August 15 were made at the center of the eastward moving corridor (Fig. 5 right). A more detailed description of the survey flights for the individual days is given in the Appendix. Finally, the weather during the last week of the campaign was characterized by unfavorable flight conditions again. A low-pressure cell slowly moving up Fram Strait led to strong northerly winds at Station Nord in combination with precipitation (snow fall and rain). After the temporal closure of the runway, Polar 6 departed to Longyearbyen on August 21, 2022.

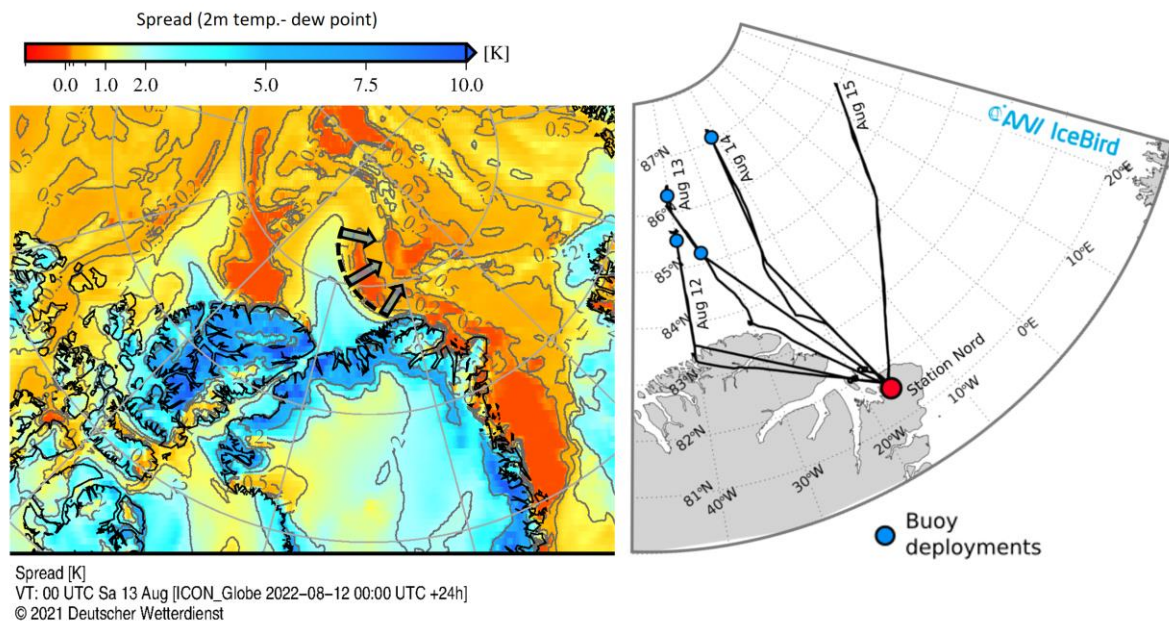


Fig 5: A corridor of suitable surveying conditions (absence of fog and low-level clouds) opened up on August 11. Left: shows the forecasted spread (air temperature at 2m minus dew point) for August 13 from the ICON model. Over the course of the next four days, the corridor slowly moved eastward (black arrows). During this short and favorable period, all survey flights were carried out. Right: Panel provides an overview of the survey flights (black lines). Positions where buoys (CALIBs) were deployed are highlighted in blue.

Tab. 1: Overview of different survey and ferry flights carried out between July 12 and August 24, 2022. For survey flights, the list of active sensors is provided.

| Airport Codes | |
|----------------------|-------------------------|
| ENSB | Longyearbyen, Svalbard |
| BGNO | Station Nord, Greenland |
| CYLT | Alert, Canada |
| TOS | Tromsø, Norway |
| TRD | Trondheim, Norway |
| EDDW | Bremen, Germany |

| Sensor Codes | |
|---------------------|---|
| AEM | Airborne Electromagnetic Sensor (EM-Bird) |
| MACS | MACS DLR Kamera System (optical + NIR) |
| HC | Hyperspectral Camera, Specim AisaEAGLE and AisaHAWK |
| LS | Laserscanner, Rigl (VQ580) |
| NI | Nikon Camera (Fisheye) |
| SP | Spectrometer (Ocean Optics, NIRQuest) |
| CBD | Calib Buoy Deployment |

| Schedule | | | | | |
|---------------------------------------|--------------|-----------------|-----------------|--------------------|--------------------------------|
| Date | Route | Type | Air Time | Flight time | Active sensors |
| Jul 12, 2022 | EDDW-EDDW | Test flight | 1.6 | 1.7 | AEM, MACS, HC, LS, NI, SP |
| Jul 13, 2022 | EDDW-EDDW | Training Flight | 4.3 | 4.5 | MACS, HC, LS, NI |
| Aug 01, 2022 | EDDW-TRD | Ferry flight | 3.5 | 3.7 | None |
| Aug 02, 2022 | TRD-ENSB | Ferry flight | 4.8 | 5 | None |
| Aug 04, 2022 | ENSB-BGNO | Ferry flight | 2.3 | 2.5 | None |
| Aug 12, 2022 | BGNO-BGNO | Survey flight | 5.9 | 6.6 | AEM, HC, LS, CBD, NI, SP |
| Aug 13, 2022 | BGNO-BGNO | Survey flight | 5.8 | 5.9 | AEM, MACS, HC, LS, CBD, NI, SP |
| Aug 14, 2022 | BGNO-BGNO | Survey flight | 5.3 | 5.5 | AEM, MACS, HC, LS, CBD, NI, SP |
| Aug 15, 2022 | BGNO-BGNO | Survey flight | 5.4 | 5.5 | AEM, MACS, HC, LS, CBD, NI, SP |
| Aug 20, 2022 | BGNO-BGNO | Survey flight | 4.7 | 4.9 | MACS, LS, HC, NI |
| Aug 21, 2022 | BGNO-ENSB | Ferry flight | 2.3 | 2.5 | None |
| Aug 24, 2022 | ENSB-EDDW | Ferry flight | 9 | 9.2 | None |
| Total flight hours | | | 54.9 | 57.5 | |
| Ferry time | | | 21.9 | 22.9 | |
| Survey time (incl. training and test) | | | 33 | 34.6 | |

4.0 Preliminary Results

A total of 830 km of ice thickness profile data, and around 1700 km of laser surface scans and optical images were recorded despite difficult flight conditions. Figure 6 (left, a) shows the location of the survey flights carried out in 2022 (red) together with previous flights from the years 2001 to 2021 (black). Based on satellite data and an approach called IceTrack (Krumpen et al. 2020), the survey ice was traced back in time to the area where it was formed. Using this method, the observed ice thicknesses and surface properties can be related to its age and other processes that affected the ice on its drift through the Arctic (Krumpen et al. 2020). Below we present some preliminary results from this approach: Figure 6 (right, a) shows the drift trajectories and age of the surveyed sea ice. The region in which survey flights were carried out was dominated by SYI (second year ice) and/or MYI (multi-year ice). Surface temperatures derived along track from reanalysis data (NCEP, Kanamitsu et al. 2002) indicate that the ice has been exposed to rather average winter and summer temperatures over its lifetime (not shown). A marked difference from previous years is that Fram Strait ice in August 2022 did not originate in the Russian Arctic, as is often the case, but was mostly formed in the central Arctic.

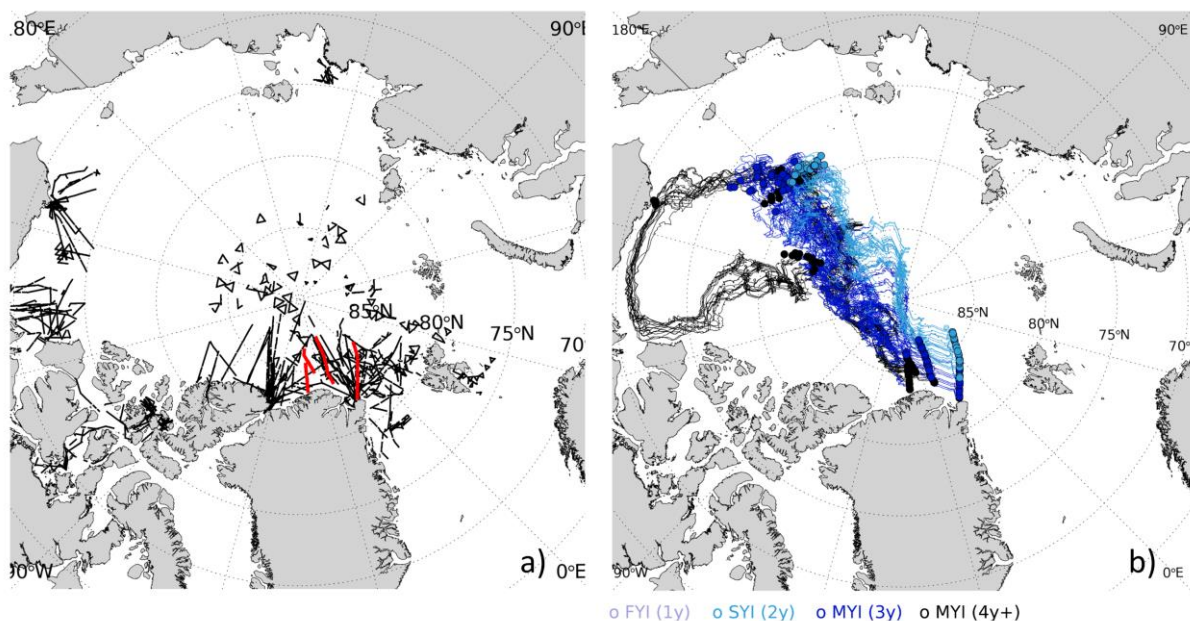
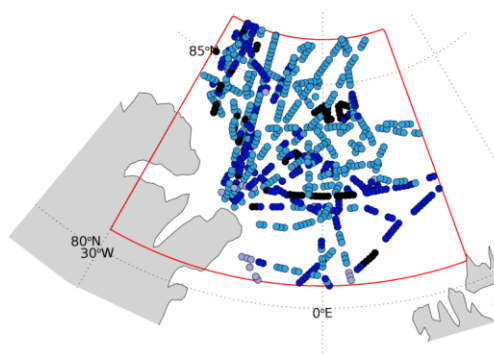


Fig. 6 a): Sea ice thickness surveys carried out by AWI in the Arctic between 2001 and 2021 (black lines) and in August 2022 (IceBird, red lines) using airplanes and helicopters. The sea ice thickness is determined with the EM-Bird, an electromagnetic sensor that is "towed" over the ice at a height of 15 meters by airplane or helicopter.

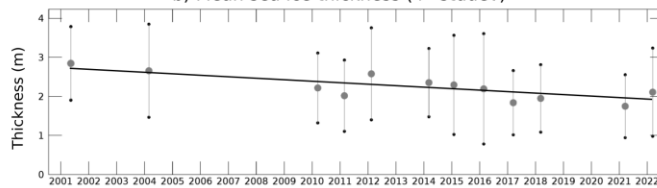
Fig. 6 b): Drift (colored lines) and origin of the sea ice surveyed in August 2022. The color of the trajectories correspond to the age of the surveyed ice.

Figure 7 shows the variability and changes in sea ice thickness in Fram Strait and surrounding areas. The figure includes data from all campaigns over the past two decades in which measurements within the region (red box after Belter et al. 2021) were obtained during the summer months (July and August). Accordingly, the modal (about 1.5 m) and mean (about 2.1 m) ice thicknesses measured in August 2022 roughly correspond to the average of the past 11 years (2010 - 2021). Thus, similar to the sea ice extent in August 2022, the ice thickness decrease is also relatively moderate this year. However, the trend toward steadily decreasing mean and modal ice thickness continues in 2022.

a) Survey flights between Jul/Aug. 2001 - 2022



b) Mean sea ice thickness (+- stddev)



c) Modal sea ice thickness (+- stddev)

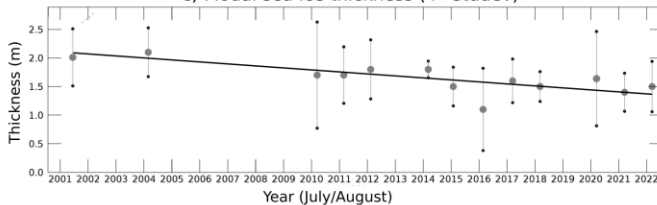


Fig. 7: a) Ice thickness measurements obtained in summer (July and August) between 2001 and 2022 in Fram Strait and adjacent areas (red box after Belter et al. 2021). Color coding corresponds to ice age (see Figure 6b). In b) and c), the mean and modal ice thicknesses of the flights from the respective years are shown. The mean and modal ice thicknesses in summer 2022 are 2.1 and 1.5 m, respectively.

The evaluation of laser distance measurements, which can be used to make assumptions about the frequency of pressure ridges and sails, also show no conspicuous values: On average, 8.6 pressure ridges were identified per flight kilometer. The mean ridge/sail occurrence over the past 11 years is 8.2 n/km. Noticeable in 2022 was a relatively low melt ponds coverage along most of the survey flights. Precise quantification of the melt pond fraction based on optical data is still pending.

Appendix: Survey Flight Descriptions

Below we provide for every day when survey flights were made

- specific flight information and problems encountered (if any)
- the flight track and auxiliary data

Air time/flight time, list of active sensors etc. is provided in Table. 1.

Survey flight August 12, 2022

Specific flight information and problems encountered (if any)

An AEM-Bird survey flight was carried out from the northern tip of Greenland (82° 2' N) along a corridor of suitable low-level cloud conditions (see Fig. A1) towards 85°30' N. Optical and laser scanner systems were operated simultaneously. On the way back (same transect line), the survey altitude was set to 2000ft. Activities on the way back were limited to the hyperspectral camera and the laser scanner system. The MACS camera system failed to initiate. At the northern most point of the survey line, a CALIB buoy was deployed (IMEI 300234066893240).

Before landing, optical sensor and laser scanner calibrations were carried out in the vicinity of Station Nord and over the runway.

August 12, 2022

Weather conditions: VIS/VIIRS from satellite (red color indicates ice sfc.)

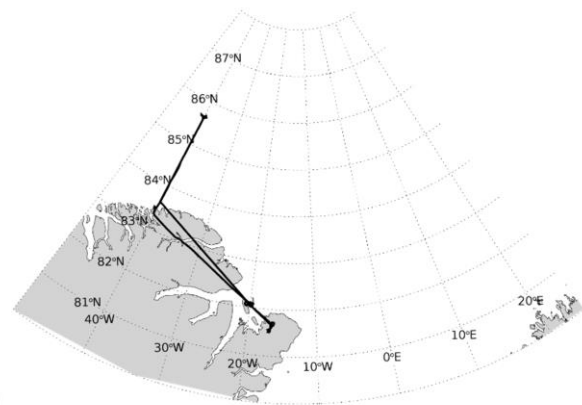
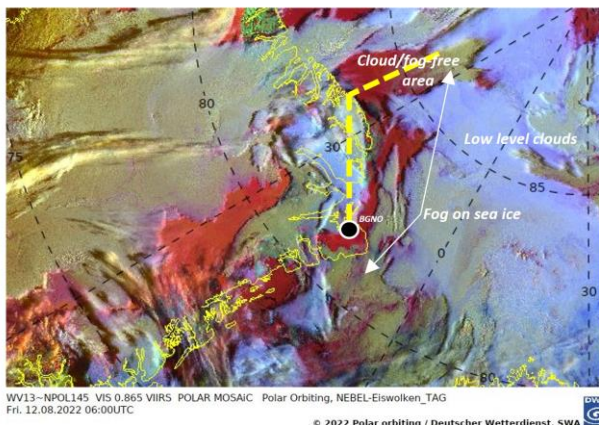


Fig. A1: Planned (left, yellow dotted line) and completed (right, black line) survey flight on August 12, 2022. Planning was done based on satellite information provided by DWD.

Survey flight August 13, 2022

Specific flight information and problems encountered (if any)

Stable and cloud/fog-free weather conditions and southerly winds at Station Nord enabled us to continue surveying activities over sea ice north of Greenland. The AEM-Bird survey started not at the fast ice edge as originally planned, but further offshore at 84°30'N, 31°W due to a fog bank that developed unexpectedly on the downwind side of the Wandel polynya. The survey went towards 86°30'N, 40W. Optical and laser scanner systems were operated simultaneously to the AAEM-Bird. At the northern most point of the survey line, a CALIB buoy was deployed (IMEI 300234066890230 at 86°09'N, 40°40'W). The hyperspectral camera, laser scanner and MACS measurements were made at 2000ft on the way back, including an additional CALIB deployment (IMEI 300234066893240 at 85°33'N, 37°17'W).

Before landing, another optical sensor calibration was carried out in the vicinity of Station Nord.

August 13, 2022

Weather conditions: VIS/VIIRS from satellite (red color indicates ice sfc.)

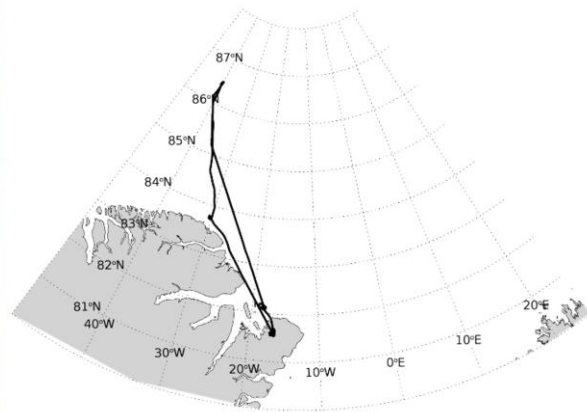
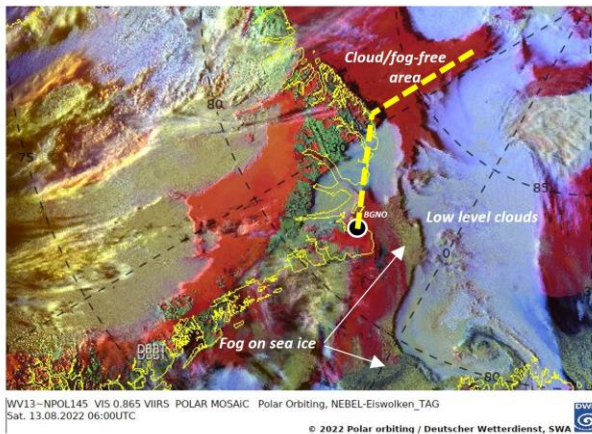


Fig. A2: Planned (left, yellow dotted line) and completed (right, black line) survey flight on August 13, 2022. Planning was done based on satellite information provided by DWD.

Survey flight August 14, 2022

Specific flight information and problems encountered (if any)

We started with a ferry flight over a patch of low-level clouds and fog banks in the northeast of Station Nord. Surveying with the AEM-Bird started at 83°40'N, 23°W and went until 87°10'N, 22°W following the edge of a fog bank. Optical and laser scanner systems were operated simultaneously to the AEM-Bird. At the northernmost point, a CALIB buoy was deployed (IMEI 300234066896220 at roughly 87°N, 22°W). The way back (same transect line) was flown at 2000ft while doing hyperspectral camera, laser scanner and MACS measurements. No system failures observed, except one laser scanner failure during the AEM-Bird survey on the way out.

August 14, 2022

Weather conditions: VIS/VIIRS from satellite (red color indicates ice sfc.)

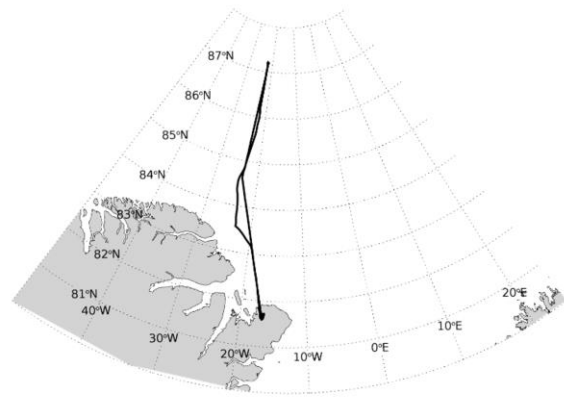
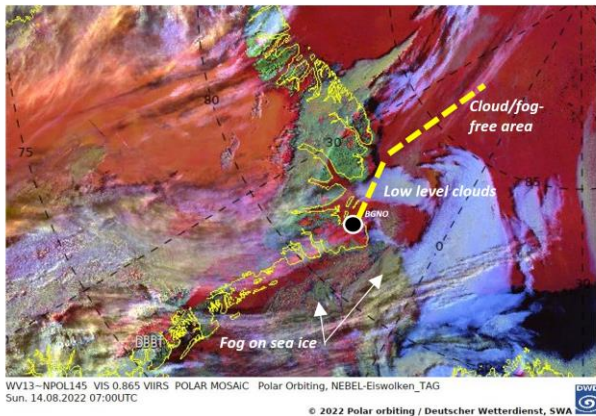


Fig. A3: Planned (left, yellow dotted line) and completed (right, black line) survey flight on August 14, 2022. Planning was done based on satellite information provided by DWD.

Survey flight August 15, 2022

Specific flight information and problems encountered (if any)

The AEM-Bird survey started at the fast ice edge near Station Nord and went towards 84°20N, 0°E and further towards 85°50N, 15°E. Optical and laser scanner systems were operated simultaneously. The way back was made at 2000 ft (same transect) with the hyperspectral camera, laser scanner and MACS camera. No major system failures observed, except two laser scanner failures (way out) and GPS issues (way back).

August 15, 2022

Weather conditions: VIS/VIIRS from satellite (red color indicates ice sfc.)

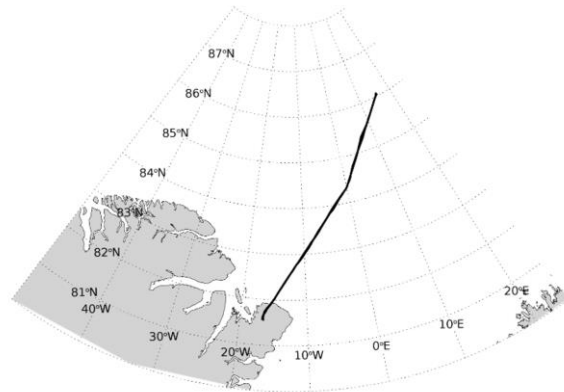
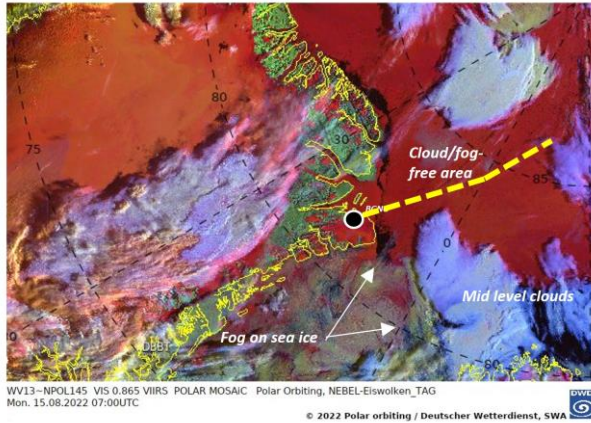


Fig. A5: Planned (left, yellow dotted line) and completed (right, black line) survey flight on August 15, 2022. Planning was done based on satellite information provided by DWD.

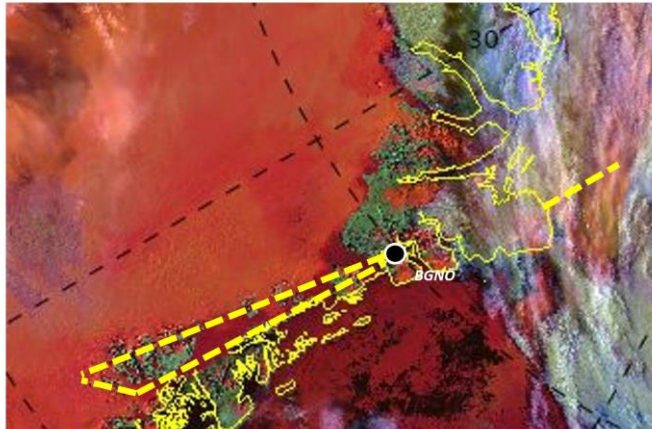
Survey flight August 20, 2022

Specific flight information and problems encountered (if any)

Glacier flight with laser scanner and MACS camera system near 79°N. For specific information contact Angelika Humbert (AWI, PI). No problems encountered.

August 20, 2022

Weather conditions: VIS/VIIRS from satellite (red color indicates ice sfc.)



WV13-NPOL145 VIS 0.865 VIIRS POLAR MOSAIC Polar Orbiting, NEBEL-Eiswolken_TAG
Sat. 20.08.2022 07:00UTC
© 2022 Polar orbiting / Deutscher Wetterdienst, SWA 

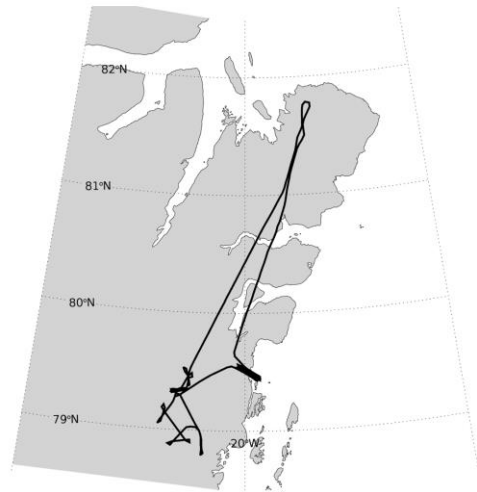


Fig. A6: Planned (left, yellow dotted line) and completed (right, black line) survey flight on August 20, 2022. Planning was done based on satellite information provided by DWD.

References

- Belter, H. J., Krumpfen, T., von Albedyll, L., Alekseeva, T. A., Birnbaum, G., Frolov, S. V., Hendricks, S., Herber, A., Polyakov, I., Raphael, I., Ricker, R., Serovetnikov, S. S., Webster, M., and Haas, C.: Interannual variability in Transpolar Drift summer sea ice thickness and potential impact of Atlantification, *The Cryosphere*, 15, 2575–2591, <https://doi.org/10.5194/tc-15-2575-2021>, 2021.
- Krumpfen, T., Belter, H. J., Boetius, A., Damm, E., Haas, C., Hendricks, S., Nicolaus, M., Noethig, E.-M., Paul, S., Peeken, I., Ricker, R., and Stein, R.: Arctic Warming interrupts the Transpolar Drift and affects long-range transport of sea ice and ice-rafted matter, *Scientific Reports*, 9, <https://doi.org/10.1038/s41598-019-41456-y>, 2019
- Landy, J., Dawson, G., Tsamados, M., Bushuk, M., Stroeve, J., Howell, S., Krumpfen, T., Babb, D., Komarov, A., Belter, J., and Heorton, H.: A year-round satellite sea ice thickness record from CryoSat-2, *Nature*, in press, [10.1038/s41586-022-05058-5](https://doi.org/10.1038/s41586-022-05058-5), 2022
- Kanamitsu, M., Ebisuzaki, W., Woollen, J., Yang, S.K, Hnilo, J.J., Fiorino, M. and G. L. Potter, NCEP-DOE AMIP-II Reanalysis (R-2): , 1631-1643, Nov 2002, *Bulletin of the American Meteorological Society*.
- Krumpfen, T., Birrien, F., Kauker, F., Rackow, T., von Albedyll, L., Angelopoulos, M., Belter, H. J., Bessonov, V., Damm, E., Dethloff, K., Haapala, J., Haas, C., Harris, C., Hendricks, S., Hoelemann, J., Hoppmann, M., Kaleschke, L., Karcher, M., Kolabutin, N., Lei, R., Lenz, J., Morgenstern, A., Nicolaus, M., Nixdorf, U., Petrovsky, T., Rabe, B., Rabenstein, L., Rex, M., Ricker, R., Rohde, J., Shimanchuk, E., Singha, S., Smolyanitsky, V., Sokolov, V., Stanton, T., Timofeeva, A., Tsamados, M., and Watkins, D.: The MOSAiC ice floe: sediment-laden survivor from the Siberian shelf, *The Cryosphere*, 14, 2173–2187, <https://doi.org/10.5194/tc-14-2173-2020>, 2020.